



A Novel Acid-Degradable PEG Crosslinker for the Fabrication of pH-Responsive Soft Materials

Iuliia Myrgorodska, Mary Jenkinson-Finch, Rafael O. Moreno-Tortolero, Stephen Mann,* and Pierangelo Gobbo*

The design and synthesis of a novel acid-degradable polyethylene glycol-based *N*-hydroxysuccinimide (NHS) ester-activated crosslinker is reported. The crosslinker is reactive towards nucleophiles and features a central ketal functional group that is stable at pH > 7.5 and rapidly hydrolyses at pH < 6.0. The crosslinker is used to (i) fabricate acid-degradable polysaccharide hydrogels that exhibit controlled degradation upon exposure to an acidic environment or via endogenous enzyme activity; and (ii) construct hydrogel-filled protein-polymer microcompartments (termed *proteinosomes*) capable of pH-dependent membrane disassembly. Taken together the results provide new opportunities for the fabrication of pH-responsive soft materials with potential applications in drug delivery, tissue engineering, and soft-matter bioengineering.

diagnostic and sensing devices,^[3] and lithography.^[4] Ketals have attracted much attention as acid-cleavable functional groups because they readily hydrolyze to the corresponding ketone and alcohols under mildly acidic conditions (Scheme 1a).^[5] Ketals display good stability under mildly alkaline or neutral conditions, tunable hydrolysis rates, and simple synthetic routes.^[6] Because of these reasons, ketals (and acetals) have been used to develop a wide range of polymers for the assembly of acid-degradable soft materials including micro- and nanocarriers,^[7] micro- and nanogels,^[6a] hydrogels,^[8] and cross-linked micelles.^[9] As a general strategy, direct radical polymerization methods are employed in which the ketal-

containing monomer is directly incorporated into the polymer backbone or used as a crosslinking moiety, thus providing a handle for effective and controllable acid-mediated material degradation or cargo-release.^[10]

However, to the best of our knowledge, the possibility of directly using a ketal-containing crosslinker capable of reacting through bioconjugation or click chemistry for the generation of chemically crosslinked acid-degradable soft materials has not been explored. One of the most common, versatile and effective bioconjugation techniques for crosslinking involves the reaction of primary amines with *N*-hydroxysuccinimide (NHS) esters. Therefore, devising a strategy for the synthesis of an acid-degradable water-soluble NHS-activated crosslinker would open up important new avenues in smart materials chemistry.


Herein, we report the synthesis of a novel versatile polyethylene glycol (PEG)-based NHS ester-activated ketal crosslinker that is reactive towards nucleophiles, stable at pH > 7.5 and rapidly cleaves at pH < 6.0. We showcase the use of the new crosslinker for the fabrication of acid-degradable carboxymethyl chitosan (CM-chitosan) hydrogels and nanometer-thick semi-permeable protein-polymer microcapsules, termed *proteinosomes*, that are commonly used as a synthetic protocell model.^[11] The controlled degradation of these soft materials is triggered either by direct exposure to an acidic environment or by endogenously decreasing the pH via internalized glucose oxidase (GOx) activity. In both approaches, consequent hydrolysis of the ketal crosslinker results in either complete dissolution of the CM-chitosan hydrogel or disassembly of the proteinosome membrane. Taken together our results offer a new route to the fabrication of pH-responsive soft materials with potential

1. Introduction

The fabrication of stimuli-responsive materials has undergone significant advances in recent years due to the development of new synthetic methods in polymer science.^[1] Among numerous types of external stimuli, pH is a particularly attractive target because of its simplicity and biological relevance. Smart pH-responsive materials respond to pH changes in the environment by altering their physicochemical properties or via the cleavage of covalent bonds. The latter strategy has found applications in bio-related areas such as drug-delivery systems,^[2]

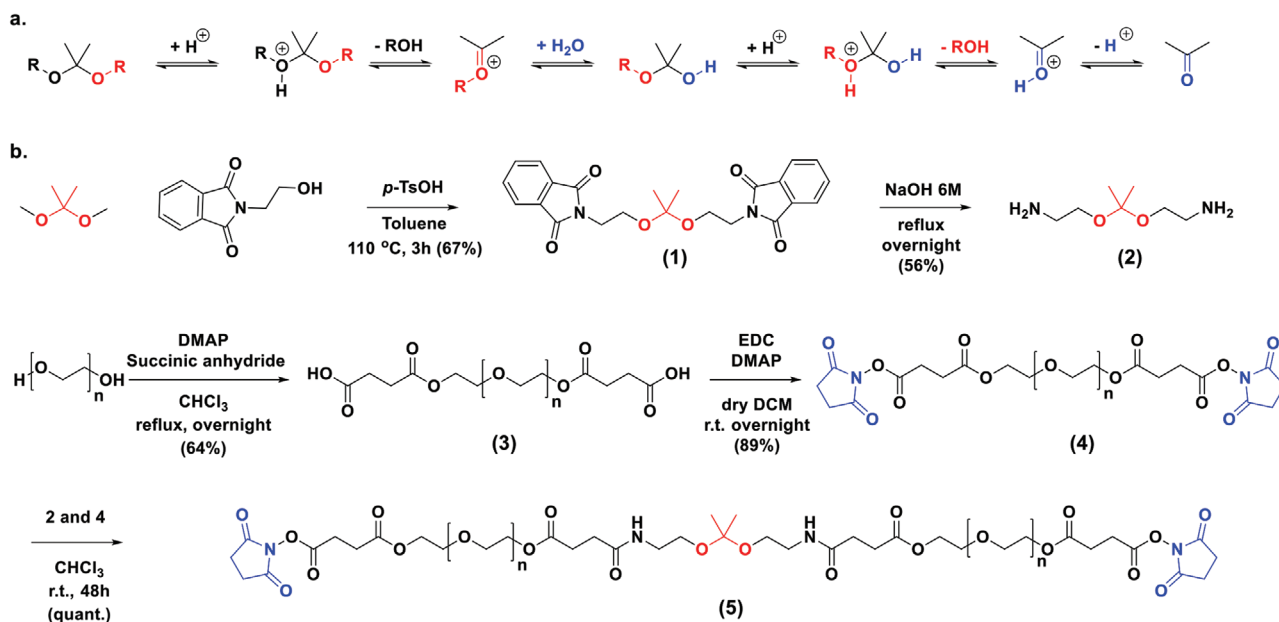
Dr. I. Myrgorodska, M. Jenkinson-Finch, Prof. S. Mann
 Centre for Protolife Research and Centre for Organised Matter Chemistry
 School of Chemistry
 University of Bristol
 Bristol BS8 1TS, UK
 E-mail: s.mann@bristol.ac.uk

R. O. Moreno-Tortolero, Dr. P. Gobbo
 School of Chemistry
 University of Bristol
 Bristol BS8 1TS, UK
 E-mail: pierangelo.gobbo@bristol.ac.uk

 The ORCID identification number(s) for the author(s) of this article can be found under <https://doi.org/10.1002/marc.202100102>.

© 2021 The Authors. Macromolecular Rapid Communications published by Wiley-VCH GmbH. This is an open access article under the terms of the Creative Commons Attribution License, which permits use, distribution and reproduction in any medium, provided the original work is properly cited.

DOI: 10.1002/marc.202100102



Scheme 1. a) Scheme showing the well-established hydrolysis mechanism of ketals. The rate-determining step is considered to be the formation of the resonance-stabilized carboxonium ion intermediate. b) Synthetic route to the preparation of the acid-degradable crosslinker (5). The acid-sensitive ketal moiety is highlighted in red, whereas the two terminal amine-reactive NHS ester-activated functional groups are highlighted in blue.

future applications in drug delivery, synthetic protobiology, tissue engineering, and soft-matter bioengineering.

2. Results and Discussion

Synthesis of the PEG-based acid-degradable crosslinker (5) was undertaken in five steps (Scheme 1b; Section S1.2, Supporting Information) involving the synthesis of the acid-degradable ketal-diamine core (2; 2,2-bis(aminoethoxy)propane; Figures S1 and S2, Supporting Information) and separately the synthesis of the activated polyethylene glycol linking unit (4; *O,O'*-bis[2-(*N*-succinimidyl-succinate)]polyethylene glycol, PEG-diNHS) from bis(succinic acid ester)polyethylene glycol (3; $M_n = 1000$ Da; ≈ 22 ethylene glycol monomers units) (Figures S3–S6, Supporting Information). Reaction of (4) and (2) in a 2:1 molar ratio yielded (5) in quantitative yield. The overall yield of the five-step synthetic sequence was 21%. The ^1H NMR spectrum of compound (5) showed the presence of the ketal peak at 1.33 ppm, the presence of the NHS methylene protons peak at 2.84 ppm, and a twofold increase of the PEG peak at 3.63–3.71 ppm (Figures S7 and S8, Supporting Information). MALDI-TOF mass spectrometry also confirmed the coupling of two polymer chains of (4) to a single acid-degradable core (2) (Figure S9, Supporting Information). Crosslinker (5) was found to be stable for several months if stored at -20 °C and under an inert atmosphere and was used directly without any additional purification steps.

The hydrolysis kinetics of crosslinker (5) in deuterated phosphate buffer solution (PBS) as a function of pH were investigated to gain critical information for designing experimental methodologies for the fabrication of novel acid-degradable soft materials. ^1H NMR spectroscopy was used to track the disappearance of the ketal peak at 1.33 ppm and concomitant appearance

of the acetone peak at 2.22 ppm over time when molecule (5) was exposed to pH values between 5.0 and 8.5, according to the reaction mechanism reported in Scheme 1a. Since ketal hydrolysis follows a pseudo-first order kinetics, k_{obs} values and half-life times were calculated from the integrals of the same two signals according to the method reported in Section S1.3 (Supporting Information). Significantly, we observed that at $\text{pH} > 7.5$ the crosslinker remained stable in solution (reaction monitored for more than 1 week), whereas hydrolysis became more prominent as the pH decreased. More specifically, between pH 6.0 and 7.5 the half-life times of (5) ranged from 16 min to 9 h, respectively, whereas at pH 5.5 and 5.0 the half-life times were of 2.1 and 3.7 min, respectively (Figure 1; Figure S10, Supporting Information). Liu and Thayumanavan has previously reported a half-life time of 32 h for the phthalimide-substituted ketal intermediate (1) at pH 5.^[6a] Such a marked difference in crosslinker stability between the intermediate (1) and final product (5) is consistent with an increasing electron donating character of the adjacent amine groups.

The high stability of (5) at $\text{pH} > 7.5$ and its fast kinetics of hydrolysis at $\text{pH} < 6.0$ make the PEG-based derivative very attractive as an acid-degradable crosslinker for applications in soft materials chemistry. In particular, given the pH-sensitive properties of (5), we anticipated that its reaction with amine-functionalized polysaccharides and proteins would lead to a new approach for the formation of acid-degradable chemically crosslinked biomaterials.

To showcase this, we prepared six different samples of polysaccharide hydrogels by mixing 5 μL of an aqueous solution of (5) (0, 1, 2.5, 5, 10, or 20 mg) with 190 μL of an aqueous solution of CM-chitosan (40 mg mL^{-1}) containing 5 μL of a commercial solution of universal indicator. The solutions were mixed vigorously for 20 s, and a sol–gel transition occurred in

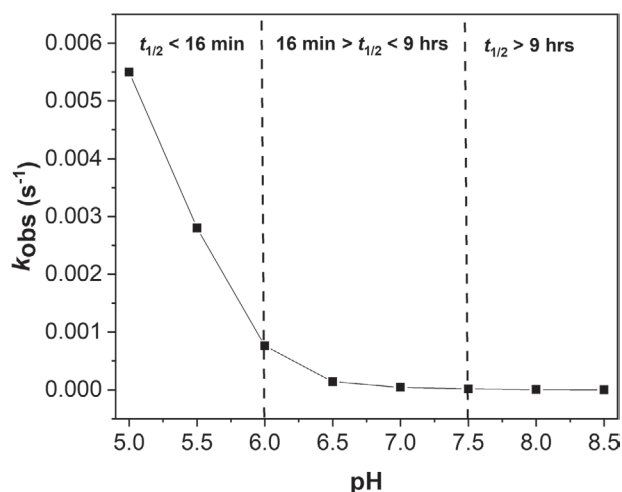


Figure 1. Plot of the pseudo-first order rate constants, k_{obs} , determined for the hydrolysis of crosslinker (5) over a range of pH values. The dashed vertical lines highlight three different pH regions where the acid-degradable crosslinker (5) hydrolyses in less than 16 minutes (left, $\text{pH} < 6.0$), hydrolyses in 16 min to 9 h (middle, $6.0 > \text{pH} < 7.5$), and shows good stability for more than 9 h (right, $\text{pH} > 7.5$).

less than 30 min for samples containing greater than 2.5 mg of (5) (Figure 2). Crosslinked CM-chitosan hydrogels were analyzed using linear and transient rheology. Initially, strain and frequency sweeps were carried out in oscillatory mode to determine the linear viscoelastic region of a representative CM-chitosan hydrogel prepared by mixing 1.5 mL of a solution of CM-chitosan 40 mg mL^{-1} with 15 mg of crosslinker (5). The linear viscoelastic region of the hydrogel was identified to be between 0.01% and 250% of shear strain and between 0.01 and 10.00 Hz, with the elastic modulus (G') being independent of frequency and at least one order of magnitude higher than the viscous modulus (G'') (Figures S11 and S12, Supporting Information). The linear viscoelastic region was assumed to be the same for other hydrogel samples prepared using higher amounts of crosslinkers.

The crosslinking kinetics associated with formation of the pH-degradable hydrogels was studied using transient analysis methods at values within the determined linear viscoelastic region of the hydrogels (10% strain and 1.00 Hz frequency). Pregel solutions were prepared by quickly mixing 975 μL of aqueous CM-chitosan (40 mg mL^{-1}) with 25 μL of an aqueous solution of (5) (15, 20, or 30 mg). An oscillatory stimulation at 10% shear strain and 1.00 Hz was then immediately applied for 50 min. In all samples G'' was initially higher than G' confirming the liquid nature of the samples. As time evolved, G' increased more than G'' indicating progressive formation of a cohesive network. The gelation point, defined as the crossover point between the curves of the elastic and viscous moduli, was found to decrease linearly with increasing amount of crosslinker (Figure S13a, Supporting Information). In all samples both G' and G'' moduli continued to evolve until they eventually reached a plateau after ≈ 17 min, indicating the end of the gelation process. As expected, the final values of the shear moduli were found to progressively increase with increasing amounts of crosslinker (5) used to prepare the samples, indicating the

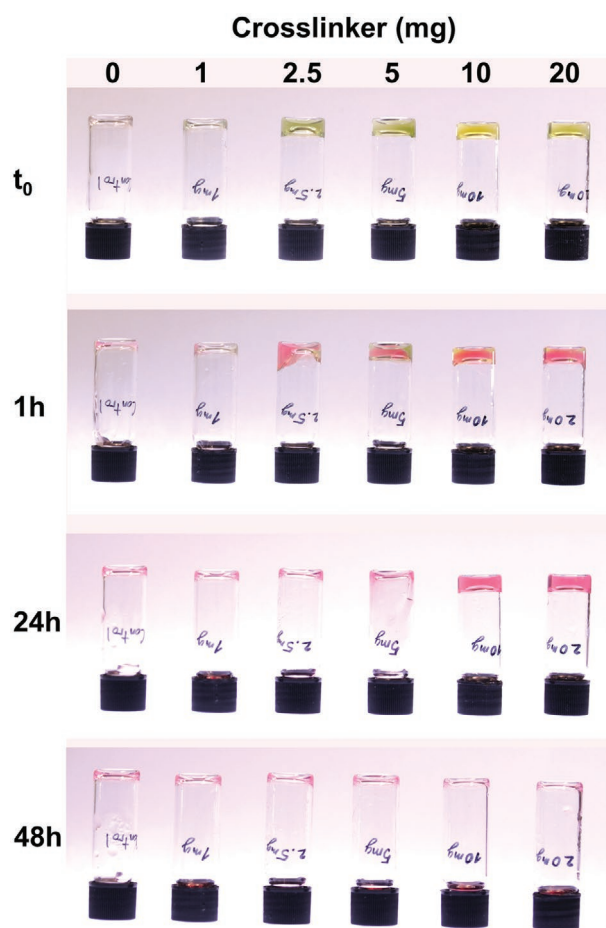


Figure 2. Time-dependent photographs of inverted vials containing CM-chitosan hydrogels (4 wt%, 190 μL) crosslinked with different amounts of crosslinker (5) ranging from 0 to 20 mg as specified at the top of the figure. The top photograph (t_0) shows the presence of the hydrogel at the beginning of the experiment. The hydrogels were then exposed to 5 μL of HCl (1 M) and photographs were acquired after 1, 24, and 48 h, as indicated on the left-hand side of the figure. The hydrogels were preloaded with a universal indicator, which showed an alkaline pH at t_0 (top row, yellow color) and acidic pH (pink color) after addition of HCl. The latter gave rise to hydrolysis of crosslinker (5) and disassembly of the hydrogel at a rate that depended on the crosslinker concentration.

formation of stiffer hydrogels (Figure S13b, Supporting Information). Taken together these observations indicate that the acid degradable crosslinker (5) can be successfully employed to fabricate hydrogels via chemical crosslinking with amine-functionalized high molecular weight polymers.

Acid-promoted degradation of the crosslinked CM-chitosan hydrogels was undertaken by direct addition of hydrochloric acid (HCl, 1.0 M) to samples prepared as above in small vials (2 mL). Hydrogels generated using 12.5 or 25 mg of crosslinker (5) fully disassembled in ≈ 2 h, whereas hydrogels prepared using 50 and 100 mg mL^{-1} of (5) degraded in 48 h, indicating an inverse proportionality to the extent of chemical crosslinking. In all samples, before acid addition the pH of the hydrogel was 8.0 and after complete disassembly the pH of the solution was 2.0. In contrast, the hydrogels remained stable for over a week in control experiments conducted under the same conditions

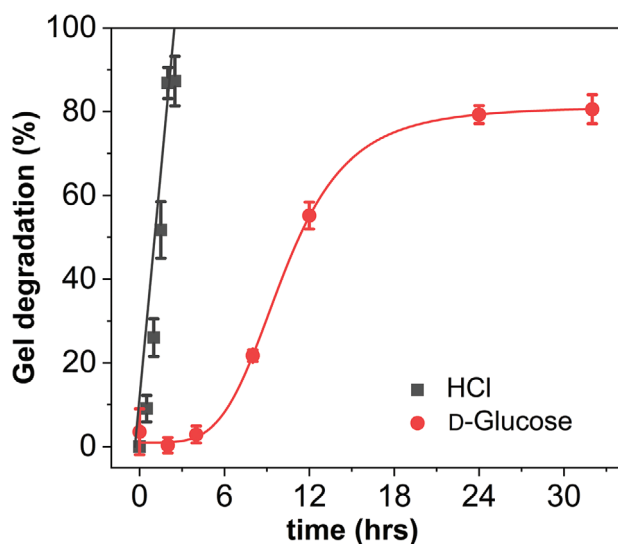


Figure 3. Graph comparing the time-dependent acid-mediated hydrogel degradation as determined from freeze-drying/weighing for CM-chitosan hydrogels (4 wt%, 200 μ L) crosslinked with 3 mg of crosslinker (5) and directly exposed to 300 μ L of HCl 1 M (black plot), or preloaded with 0.5 mg of GOx and exposed to 300 μ L of D-Glucose 0.5 M (red plot). Experiments were repeated in triplicate, error bars indicate standard deviation.

but using the pH-stable crosslinker PEG-diNHS in place of (5) (Figure S14, Supporting Information). A quantitative study of the time-dependence of acid-mediated hydrogel degradation was carried out by freeze drying and weighing the residual hydrogels after exposure to HCl for various periods of time (Section S1.5, Supporting Information). The data showed that under the conditions employed, hydrogel degradation started immediately after addition of the acid and continued linearly over a period of \approx 2 h (Figure 3).

Alternatively, we co-crosslinked GOx inside the acid-degradable CM-chitosan hydrogels as an endogenous trigger of acid-mediated hydrogel disassembly.^[12] The GOx-containing hydrogel was exposed to an aqueous solution of D-glucose (0.5 M), which slowly permeated through the hydrogel where it was progressively oxidized to gluconolactone by GOx in the presence of dioxygen. Hydrolysis of gluconolactone to gluconic acid within the hydrogel progressively decreased the pH to 4.5, causing hydrolysis of crosslinker (5) and disassembly of the hydrogel. Under these conditions, quantitative measurements showed that the GOx-containing hydrogel started to degrade after 4 h and reached a plateau level of 80% disassembly after 18 h from the addition of glucose (Figure 3). We attributed the relatively long induction time to the slow permeation of glucose through the hydrogel and the slow hydrolysis of gluconolactone to gluconic acid within the hydrogel.^[12] Furthermore, incomplete disassembly even after 30 h suggested that GOx activity was curtailed over long periods of time possibly by the increasing acidity of the hydrogel environment^[13] and depletion of the substrate. Overall, these results show that crosslinker (5) can be successfully employed to fabricate novel functional hydrogels that can be specifically engineered using GOx-mediated catalysis for programmable degradation in the presence of glucose.

Given the above observations, we sought to exploit the new amine-reactive crosslinker for the stabilization and controlled disassembly of vesicle-like nanometer-thick membranes based on the interfacial assembly of partially hydrophobic protein-polymer nanocomposites into intact semipermeable microcapsules called *proteinosomes*.^[11f] To achieve this, we synthesized aqueous suspensions of RITC-labelled bovine serum albumin (BSA)/poly(*N*-isopropylacrylamide) (PNIPAm) nanoconjugates (Section S1.6 and Figures S15 and S16, Supporting Information)^[11f] and used these along with aqueous alkaline solutions of the acid-degradable crosslinker (5) in Na₂CO₃ buffer (pH 8.5) and CM-chitosan (pH 8.5–9) to prepare water-in-oil Pickering emulsions. The droplets were incubated for 48 h to facilitate reaction of (5) with the primary amine groups of CM-chitosan as well as the RITC-labelled BSA/PNIPAm nanoconjugates present both at the droplet surface and within the interior. Fluorescence microscopy imaging showed hydrogelled droplets with an average diameter of 11 ± 6 μ m and homogeneous red fluorescence (Figure 4a,c). The droplets were subsequently transferred into Na₂CO₃ buffer (10×10^{-3} M, pH 8.5) using dialysis (Section S1.7, Supporting Information) to produce an aqueous dispersion of swollen hydrogel-containing proteinosomes with diameters of 29 ± 10 μ m (Figure 4b,c). Interestingly, if smaller amounts of crosslinker (5) were used no proteinosomes formed, whereas if larger amounts of crosslinker (5) were used proteinosomes were found to aggregate into cluster when transferred into water. By using fluorescein isothiocyanate (FITC)-labelled CM-chitosan (green fluorescence) and rhodamine B isothiocyanate (RITC)-BSA/PNIPAm nanoconjugates (red fluorescence) we were able to map the location of these crosslinked components in the intact proteinosomes using fluorescence confocal microscopy. The images indicated that the proteinosomes comprised a hydrogel-filled core of FITC-tagged CM-chitosan and excess RITC-tagged BSA/PNIPAm nanoconjugate, and a well-defined outer membrane of RITC-tagged BSA/PNIPAm nanoconjugates (Figure 4d). Crosslinking of both the core and membrane gave rise to proteinosomes that remained structurally stable for several days when stored in Na₂CO₃ buffer (10×10^{-3} M, pH 8.5).

In contrast, proteinosomes prepared without the CM-chitosan hydrogel core often fractured during transfer from oil into water.

The pH-responsive properties of the hydrogel-filled proteinosomes were studied by fluorescence microscopy and fluorescence-activated cell sorting (FACS). Visual confirmation of proteinosome disassembly in the presence of HCl (250×10^{-3} M) was obtained using time-dependent fluorescence microscopy imaging.

Figure 5a,b and Video S1 (Supporting Information) show that the total red fluorescence intensity associated with the hydrogel-containing microcapsules decayed over time, indicating progressive disassembly of the protein-polymer membrane and CM-chitosan hydrogel core within \approx 1.5 h. In contrast, a control experiment performed under the same conditions but using the pH-stable PEG-diNHS crosslinker instead of acid-degradable (5), did not reveal any significant changes in the red fluorescence intensity of the proteinosomes (Figure 5b). This indicated that possible photobleaching of the RITC tags by the laser of the fluorescence microscope had minimal effects

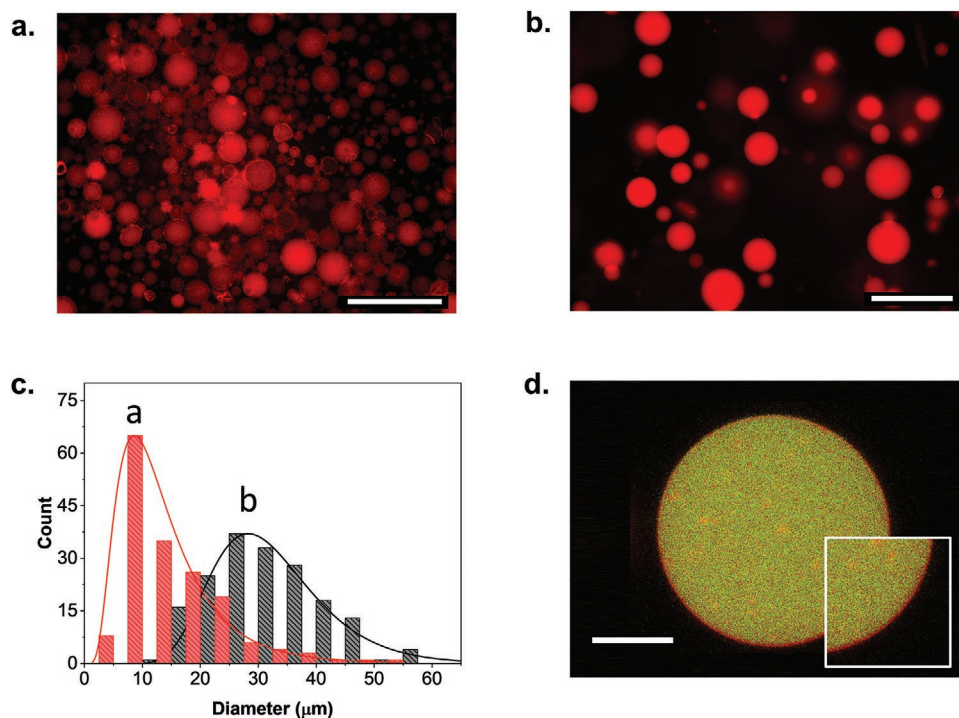


Figure 4. Fluorescence microscopy characterization of pH-sensitive hydrogel-filled proteinosomes. a) Fluorescence microscopy image of pH-sensitive hydrogel-filled proteinosomes in oil. The proteinosomes are water-in-oil (w/o) Pickering emulsion droplets stabilized by RITC-tagged (red fluorescence) BSA/PNIPAm nanoconjugates and filled with a CM-chitosan hydrogel. The proteinosome membrane as well as the CM-chitosan hydrogel are both chemically crosslinked in situ with crosslinker (5). Scale bar = 100 μm . b) Fluorescence microscopy image of the pH-sensitive hydrogel-filled proteinosomes in (a) after transfer into Na_2CO_3 buffer (10×10^{-3} M, pH 8.5). Scale bar = 100 μm . c) Graph comparing the size distribution of the pH-sensitive hydrogel-filled proteinosomes in oil shown in (a) (red plot) and the size distribution of the same proteinosomes after transfer into Na_2CO_3 buffer shown in (b) (black plot); the increase in size is associated with swelling of the inner hydrogel upon transfer to the water medium. d) Fluorescence confocal microscopy image of a single pH-sensitive hydrogel-filled proteinosome crosslinked with crosslinker (5) and in Na_2CO_3 buffer (10×10^{-3} M, pH 8.5). The image highlights that after transfer into aqueous media, the structure of the proteinosome still comprised an external membrane of crosslinked RITC-tagged BSA/PNIPAm nanoconjugates (red fluorescence) and a hydrogel-filled core of crosslinked FITC-tagged CM-chitosan (green fluorescence) and excess RITC-tagged BSA/PNIPAm nanoconjugates. Scale bar = 20 μm . The inset highlights the presence of a well-defined crosslinked RITC-tagged BSA/PNIPAm nanoconjugate membrane.

on the time-dependent fluorescence intensity values observed experimentally, thereby confirming that disassembly of the proteinosome was mediated by acid-catalyzed hydrolysis of the crosslinker. This was confirmed statistically by FACS analysis of different samples of the acid-degradable hydrogel-filled proteinosomes after incubation in HCl (250×10^{-3} M) for different times (0–2.5 h) followed by direct injection into the instrument. Time-dependent FACS analysis confirmed a fast depletion of the proteinosome population, with the total proteinosome count decreasing to 27% of its initial value after 2.5 h of incubation in the acid (Figure 5c).

Finally, we explored the possibility of coencapsulating and crosslinking GOx inside the proteinosomes to trigger the glucose-induced endogenous decrease of pH with a consequent disassembly of the microcapsule. GOx-containing, acid-degradable and hydrogel-filled proteinosomes were assembled using the same procedure as described above, followed by incubation in a glucose solution (0.5 M) for 0 to 32 h, and analysis of the proteinosome population by FACS. A slow depletion of the proteinosome population, which reached 11% of its initial value after 32 h, was observed (Figure 5d). This was associated with the slow endogenous enzyme-mediated synthesis

of gluconolactone and subsequent hydrolysis to gluconic acid. Taken together these observations show that crosslinker (5) can be used to generate hydrogel-filled proteinosomes that are stable under alkaline conditions and can progressively degrade when the pH turns acidic. More generally, these results provide scope for the generation of novel micro-compartmentalized systems with chemically programmable capabilities.

3. Conclusion

To conclude, a novel acid-degradable NHS ester-activated PEG crosslinker based on a ketal core and reactive towards nucleophiles was prepared following a simple five-step synthetic protocol. The half-life of the ketal group was investigated across a wide range of pH values and found to be stable at $\text{pH} > 7.5$ and rapidly hydrolyze at $\text{pH} < 6.0$. The possibility of using the novel crosslinker for the generation of pH-sensitive soft materials was showcased by fabricating acid-degradable hydrogels and protein-polymer microcapsules. Both types of soft materials were stable for an indefinite time under mildly alkaline conditions and progressively degraded under acidic

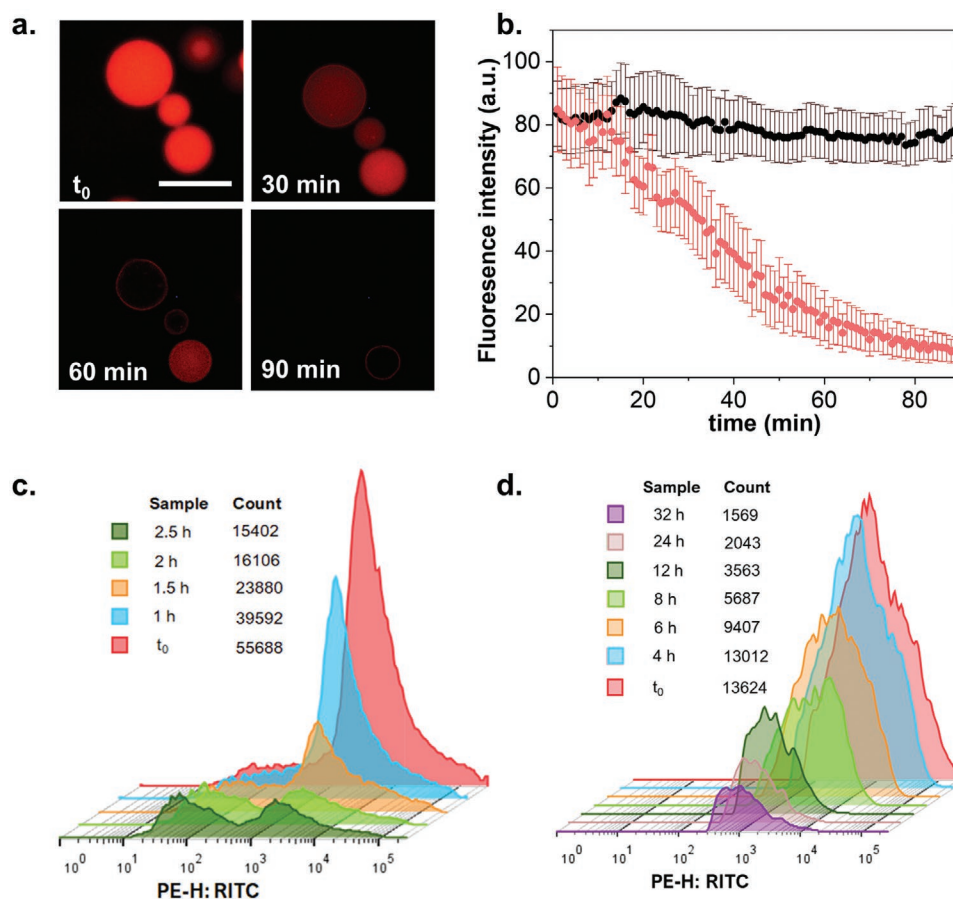


Figure 5. Time-dependent disassembly of acid-sensitive hydrogel-filled proteinosomes. a) Time-dependent fluorescence microscopy images showing a progressive decrease in red fluorescence intensity associated with the controlled disassembly of the RITC-labelled proteinosome membrane upon exposure to HCl (250×10^{-3} M). Hydrolysis of ketal crosslinker (5) results in the progressive disassembly of the crosslinked proteinosome membrane and dissolution of the encapsulated CM-chitosan crosslinked hydrogel. Scale bar = 50 μm . b) Graph comparing time-dependent changes in red fluorescence intensity for RITC-labelled hydrogel-filled proteinosomes crosslinked with acid-sensitive crosslinker (5) (red plot) or crosslinked with acid-stable PEG-diNHS crosslinker (black plot, control experiment) after exposure to 50 μL of HCl (1 M). Minimal changes in red fluorescence are observed for the control experiment. Error bars indicate standard deviation. c) Overlapped FACS-derived red fluorescence intensity (PE-H: RITC) histograms recorded for RITC-labelled hydrogel-filled proteinosomes crosslinked with crosslinker (5) and exposed to 50 μL of HCl 1 M for the different time intervals indicated. d) Overlapped FACS-derived red fluorescence intensity (PE-H: RITC) histograms recorded for RITC-labelled GOx-containing hydrogel-filled proteinosome samples crosslinked with crosslinker (5) and exposed to 50 μL of D-glucose solution (0.5 M) for the different time intervals indicated.

conditions. Importantly, we showed that the acid-mediated controlled degradation of the chemically crosslinked hydrogels and nanometer-thick proteinosome membrane could be triggered endogenously via internalized GOx activity in the presence of glucose.

From a more general perspective, to the best of our knowledge, this represents the first example of a ketal-containing crosslinker capable of directly reacting with the amine groups of biomolecules for the generation of acid-degradable soft materials. As such, we expect that the ketal-derivatized PEG crosslinker will have uses in the construction of a wide range of pH-sensitive smart materials including polymers, micelles, nanoparticles, and microcarriers, which trap and release molecular cargos on demand. Moreover, as proteinosomes are used extensively in bottom-up synthetic biology,^[11d,f,14] it should be possible to use the acid-degradable PEG crosslinker to engineer communication pathways between synthetic protocell communities that are triggered by programmable enzyme-mediated

pH decreases. Given the high reactivity towards nucleophiles, high rate of hydrolysis at pH < 6.0, and stability under mildly alkaline pH conditions, the new crosslinker could provide novel opportunities in areas such as drug delivery, synthetic protobiology, tissue engineering, soft-matter bioengineering, bioprinting, and soft robotics for the construction of acid-sensitive sensors and valves.

Supporting Information

Supporting Information is available from the Wiley Online Library or from the author.

Acknowledgements

This work was supported by the University of Bristol Vice-Chancellor's Fellowship (PG), EPSRC (New Investigator Award,

Grant Ref: EP/T01508X/1 (PG); Postgraduate Studentship (SM)), and ERC (Advanced Grant Scheme, EC-2016-ADG 740235 (SM)). The authors thank the Wolfson Bioimaging Facility for help with physical characterizations.

Conflict of Interest

The authors declare no conflict of interest.

Data Availability Statement

The data that supports the findings of this study are available in the supplementary material of this article.

Keywords

crosslinking, hydrogels, pH-mediated disassembly, proteinosomes

Received: March 1, 2021

Published online:

- [1] a) P. Rastogi, B. Kandasubramanian, *Chem. Eng. J.* **2019**, 366, 264; b) G. Isapour, M. Lattuada, *Adv. Mater.* **2018**, 30, 1707069; c) P. J. Roth, A. B. Lowe, *Polym. Chem.* **2017**, 8, 10; d) L. Y. Tan, A. C. Davis, D. J. Cappelleri, *Adv. Funct. Mater.* **2020**, 31, 2007125; e) M. W. Urban, *Handbook of Stimuli-Responsive Materials*, John Wiley & Sons, Hoboken, New Jersey, United States **2011**.
- [2] a) Y. H. Zhou, C. H. Zhou, Y. Zou, Y. Jin, S. D. Han, Q. Liu, X. P. Hu, L. Q. Wang, Y. N. Ma, Y. Liu, *Biomater. Sci.* **2020**, 8, 5029; b) L. Sun, H. Wei, X. S. Zhang, C. Meng, G. Y. Kang, W. Ma, L. W. Ma, B. Y. Wang, C. Y. Yu, *Polym. Chem.* **2020**, 11, 4469; c) Y. Ma, P. Y. He, X. H. Tian, G. L. Liu, X. W. Zeng, G. Q. Pan, *ACS Appl. Mater. Interfaces* **2019**, 11, 23948.
- [3] a) X. Su, B. X. Ma, J. Hu, T. Yu, W. H. Zhuang, L. Yang, G. C. Li, Y. B. Wang, *Bioconjugate Chem.* **2018**, 29, 4050; b) A. Srivastava, N. Amreddy, A. Babu, J. Panneerselvam, M. Mehta, R. Muralidharan, A. Chen, Y. D. Zhao, M. Razaq, N. Riedinger, H. Kim, S. R. Liu, S. Wu, A. B. Abdel-Mageed, A. Munshi, R. Ramesh, *Sci. Rep.* **2016**, 6, 38541; c) J. J. Shi, Z. Y. Chen, L. Wang, B. H. Wang, L. H. Xu, L. Hou, Z. Z. Zhang, *Acta Biomater.* **2016**, 29, 282.
- [4] M. S. Ober, D. R. Romer, J. Etienne, P. J. Thomas, V. Jain, J. F. Cameron, J. W. Thackeray, *Macromolecules* **2019**, 52, 886.
- [5] E. H. Cordes, H. G. Bull, *Chem. Rev.* **1974**, 74, 581.
- [6] a) B. Liu, S. Thayumanavan, *J. Am. Chem. Soc.* **2017**, 139, 2306; b) S. Kim, O. Linker, K. Garth, K. R. Carter, *Polym. Degrad. Stab.* **2015**, 121, 303.
- [7] a) H. U. Kim, D. G. Choi, H. Lee, M. S. Shim, K. W. Bong, *Lab Chip* **2018**, 18, 754; b) J. L. Zhao, M. H. Zhao, C. H. Yu, X. Y. Zhang, J. X. Liu, X. W. Cheng, R. J. Lee, F. Y. Sun, L. S. Teng, Y. X. Li, *Int. J. Nanomed.* **2017**, 12, 6735.
- [8] H. Pohlit, D. Leibig, H. Frey, *Macromol. Biosci.* **2017**, 17, 1600532.
- [9] D. Q. Chen, J. F. Sun, *Polym. Chem.* **2015**, 6, 998.
- [10] a) D. Q. Chen, H. B. Wang, *J. Nanosci. Nanotechnol.* **2014**, 14, 983; b) S. Binauld, M. H. Stenzel, *Chem. Commun.* **2013**, 49, 2082; c) L. Zou, Y. Shi, X. S. Cao, W. P. Gan, X. F. Wang, R. W. Graff, D. Q. Hu, H. F. Gao, *Polym. Chem.* **2016**, 7, 5512; d) Y. Y. Peng, D. Diaz-Dussan, P. Kumar, R. Narain, *Biomacromolecules* **2018**, 19, 4052; e) N. Leber, L. Kaps, M. Aslam, J. Schupp, A. Brose, D. Schaffel, K. Fischer, M. Diken, D. Strand, K. Koynov, A. Tuettenberg, L. Nuhn, R. Zentel, D. Schuppan, *J. Controlled Release* **2017**, 248, 10.
- [11] a) J. J. Su, H. X. Chen, Z. J. Xu, S. L. Wang, X. M. Liu, L. Wang, X. Huang, *ACS Appl. Mater. Interfaces* **2020**, 12, 41079; b) C. Y. Zhao, M. Zhu, Y. Fang, X. M. Liu, L. Wang, D. F. Chen, X. Huang, *Mater. Horiz.* **2020**, 7, 157; c) T. T. Wang, J. Y. Xu, X. T. Fan, X. Yan, D. Yao, R. Y. Li, S. D. Liu, X. M. Li, J. Q. Liu, *ACS Appl. Mater. Interfaces* **2019**, 11, 47619; d) P. Gobbo, A. J. Patil, M. Li, R. Harniman, W. H. Briscoe, S. Mann, *Nat. Mater.* **2018**, 17, 1145; e) X. M. Liu, P. Zhou, Y. D. Huang, M. Li, X. Huang, S. Mann, *Angew. Chem., Int. Ed.* **2016**, 55, 7095; f) X. Huang, M. Li, D. C. Green, D. S. Williams, A. J. Patil, S. Mann, *Nat. Commun.* **2013**, 4, 2239.
- [12] a) S. Pluschkell, K. Hellmuth, U. Rinas, *Biotechnol. Bioeng.* **1996**, 51, 215; b) K. Podual, F. J. Doyle III, N. A. Peppas, *J. Controlled Release* **2000**, 67, 9.
- [13] M. K. Weibel, H. J. Bright, *J. Biol. Chem.* **1971**, 246, 2734.
- [14] a) N. Martin, J. P. Douliez, Y. Qiao, R. Booth, M. Li, S. Mann, *Nat. Commun.* **2018**, 9, 3652; b) Y. Qiao, M. Li, R. Booth, S. Mann, *Nat. Chem.* **2017**, 9, 110; c) X. Huang, A. J. Patil, M. Li, S. Mann, *J. Am. Chem. Soc.* **2014**, 136, 9225.